



# THE UNIVERSITY *of* EDINBURGH

## Edinburgh Research Explorer

### Test at elevated temperature on RC beams strengthened with NSM FRP bars bonded with cementitious grout

**Citation for published version:**

Del Prete, I, Bilotta, A, Bisby, L & Nigro, E 2016, Test at elevated temperature on RC beams strengthened with NSM FRP bars bonded with cementitious grout. in 9th International Conference on Structures in Fire. Princeton.

**Link:**

[Link to publication record in Edinburgh Research Explorer](#)

**Document Version:**

Peer reviewed version

**Published In:**

9th International Conference on Structures in Fire

**General rights**

Copyright for the publications made accessible via the Edinburgh Research Explorer is retained by the author(s) and / or other copyright owners and it is a condition of accessing these publications that users recognise and abide by the legal requirements associated with these rights.

**Take down policy**

The University of Edinburgh has made every reasonable effort to ensure that Edinburgh Research Explorer content complies with UK legislation. If you believe that the public display of this file breaches copyright please contact [openaccess@ed.ac.uk](mailto:openaccess@ed.ac.uk) providing details, and we will remove access to the work immediately and investigate your claim.



## COVER SHEET

*NOTE: This coversheet is intended for you to list your article title and author(s) name only  
—this page will not appear on the CD-ROM.*

*Title: Test at elevated temperature on RC beams strengthened with NSM FRP bars  
bonded with cementitious grout*

Authors: Iolanda Del Prete<sup>1</sup>  
Antonio Bilotta<sup>2</sup>  
Luke Bisby<sup>3</sup>  
Emidio Nigro<sup>2</sup>

PAPER DEADLINE: **\*\*MARCH 11, 2016\*\***

PAPER LENGTH: **\*\*8 PAGES (Maximum) \*\***

INQUIRIES TO: **Papers to be sent to editors (*Contact Editors if further contact information necessary*).**

Dr. Maria E. Moreyra Garlock  
Associate Professor  
Princeton University

E-mail: mgarlock@princeton.edu

**Please submit your paper in Microsoft Word® format or PDF if prepared in a program other than MSWord. We encourage you to read attached Guidelines prior to preparing your paper—this will ensure your paper is consistent with the format of the articles in the CD-ROM.**

**NOTE:** Sample guidelines are shown with the correct margins.  
Follow the style from these guidelines for your page format.

Hardcopy submission: Pages can be output on a high-grade white bond paper with adherence to the specified margins (8.5 x 11 inch paper. Adjust outside margins if using A4 paper). Please number your pages in light pencil or non-photo blue pencil at the bottom.

Electronic file submission: When making your final PDF for submission make sure the box at “Printed Optimized PDF” is checked. Also—in Distiller—make certain all fonts are embedded in the document before making the final PDF.

<sup>1</sup> BuroHappold Engineering, 17 Newman Street W1T 1PD, London - UK

<sup>2</sup> Department of Structures for Engineering and Architecture, University of Naples, via Claudio 21 80125, Naples - Italy

<sup>3</sup> Institute for Infrastructure & Environment, School of Engineering, University of Edinburgh, Mayfield Road EH9 3JL, Scotland UK

## **ABSTRACT**

This paper presents the results of 12 tests on small-scale reinforced concrete beams, 1450 mm long, 150 mm wide and 150 mm deep, strengthened in flexure with a single near surface mounted (NSM) carbon FRP bar. To improve the performance at elevated temperature, the FRP bar is characterized by very high values of glass transition  $T_g$  and decomposition  $T_d$  temperature. Specific tests were performed to define the resin behavior at elevated temperature. Moreover, the FRP was bonded using a cementitious grout rather than an epoxy adhesive. The flexural tests were carried out at both ambient and elevated temperatures on both un-strengthened and strengthened beams. Tests at elevated temperature were performed using propane-fired radiant panels rather than a fire testing furnace. Two heating configurations were used: (1) localised heating near midspan only; and (2) global heating over the entire bonded length of the FRP systems. Thermo-structural response was investigated under loads typical of maximum permissible service strain conditions in the FRP. Internal temperatures, beam displacements, and slip of the FRP strengthening were measured, and strain gauges were used to measure the FRP bar strains; digital image correlation (DIC) was also used to study displacements. The tests showed the good performance of the strengthening system, both under localised and global heating, and demonstrated this cementitious grout bonded NSM CFRP strengthening system's ability to maintain structural effectiveness at temperatures up to about 600°C, under appropriate anchorage and loading conditions.

## **INTRODUCTION**

Fibre reinforced polymers (FRP) are widely applied for structural strengthening by bonding them to the exterior of reinforced concrete (RC) structures, usually with epoxy adhesives. However, degradation of mechanical properties of polymer adhesives and composites due to several environmental effects, notably including elevated temperatures, is an important factor in application of FRP composite materials in buildings and certain industrial applications. With the near surface mounted (NSM) FRP strengthening technique, the FRP bar/rod/strip is applied in a groove cut into the concrete cover of the RC member and bonded in place by filling the groove with an epoxy (or less commonly a cementitious) adhesive. Several studies

have demonstrated that NSM with epoxy adhesive exhibits superior bond behavior compared with EBR ([6], [7], [8]). NSM is also less prone to damage, since the FRP is embedded in a groove and inside adhesive. Despite this, the effectiveness of epoxy adhesive may be reduced at elevated temperatures. Ambient temperature cure epoxy adhesives are characterized by relatively low glass transition temperatures ( $T_g$ ), however higher  $T_g$  values can be achieved for pultruded FRP which is processed at elevated temperature. In NSM applications, using an elevated glass transition temperature FRP product and bonding with a cementitious grout may provide superior mechanical performance in fire, and cementitious adhesives may offer superior performance to epoxies, whilst also protecting (mechanically and thermally) the FRP, possibly without the need to apply costly and unattractive supplemental insulation materials to the exterior of the FRP strengthening system (1). Though epoxy resins are usually used as bonding agents, recently, several researchers have studied the behavior of cementitious paste or mortar bonded NSM FRP systems ([1], [3], [4], [5]).

This paper presents the results of an experimental testing program aimed at investigating the performance of a novel cementitious-bonded NSM CFRP strengthening system for concrete, which has been developed specifically to address the performance of FRP strengthening systems at elevated temperatures.

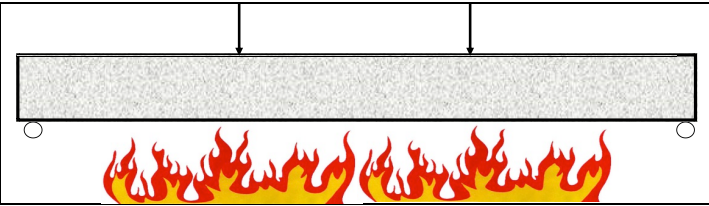
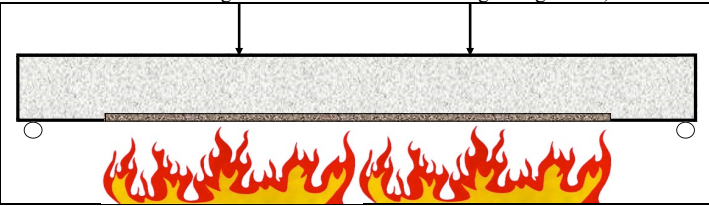
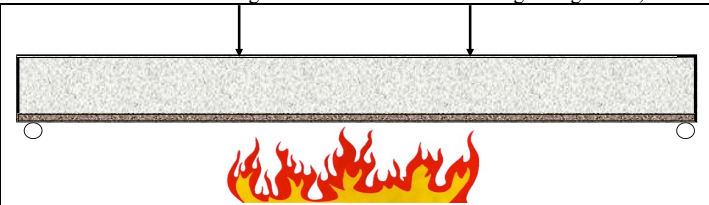
## EXPERIMENTAL PROGRAM

The experimental program consisted of six DMA and six TGA tests on the FRP bar, and twelve four-point bending tests of RC beams and NSM FRP strengthened RC beams, 1450 mm long and 150 mm square in cross-section. The flexural tests were performed both at ambient and elevated temperature. The tests at elevated temperature were executed using propane-fired radiant panels to heat the beams, rather than a standard fire-testing furnace. Two heating configurations were used: (1) localised heating near midspan only; and (2) global heating over the entire bonded length of the FRP system.

The thermo-structural response was investigated under sustained loads typical of maximum permissible service strain conditions in the FRP (Service Load (SL) = 40 kN; High Load (HL) = 50 kN). TABLE I summarizes the flexural tests, showing the relevant test beam designations.

TABLE I. EXPERIMENTAL PROGRAM

| Beam designation   | Scheme | Load    |
|--|--------|---------|
| UN-S <sub>i</sub><br>i=1,2   |        | 2mm/min |
| Note: 2 tests at ambient temperature of UN-Strengthened beams      |        |         |
| S-i<br>i=1,2,3_cut   |        | 2mm/min |
| Note: 3 tests at ambient temperature of NSM FRP Strengthened beams |        |         |

|                                     |   |                      |
|-------------------------------------|---|----------------------|
| UN-S_GloH_SL_1                      |   | SL=40 kN             |
| Note:                               | 1 test of UN-Strengthened beam in <b>Global Heating</b> configuration, under <b>Service Load</b>  |                      |
| S_GloH_SL_i<br>i=1,2                |   | SL=40 kN             |
| Note:                               | 2 tests of NSM FRP Strengthened beams in <b>Global Heating</b> configuration, under <b>Service Load</b>   |                      |
| S_LocH_SL_i<br>S_LocH_HL_i<br>i=1,2 |   | SL=40 kN<br>HL=50 kN |
| Note:                               | - 2 tests of NSM FRP Strengthened beams in <b>Localised Heating</b> configuration, with <b>Service Load</b><br>- 2 tests of NSM FRP Strengthened beams in <b>Localised Heating</b> configuration, with <b>High Load</b> |                      |

## Material Properties

Dynamic mechanic analysis (DMA) and thermogravimetric analysis (TGA) on the novel, high  $T_g$  commercial CFRP bars were conducted, to define the  $T_g$  and the  $T_d$ , respectively, of this particular FRP product.

DMA provides information about the mechanical properties of a specimen placed in sinusoidal oscillation, as a function of time ( $t$ ) and temperature, by a small sinusoidal oscillating force. The applied stress determines a corresponding strain, which is shifted with a phase shift ( $\delta$ ) due to the viscous behaviour of the polymeric material. The ratio between the stress and the strain amplitude defines the modulus of the complex modulus  $E^*$ , which is the stiffness of the material ([9], [10]).  $E^*$  is composed of the real part, the storage modulus  $E'$ , and the imaginary part, the loss modulus  $E''$ . According to [9]: the storage modulus  $E'$  represents the stiffness of a viscoelastic material; the loss modulus  $E''$  represents the viscous portion. The ratio between the loss and the storage modulus represents the loss factor  $\tan(\delta)$ . This means that a high  $\tan(\delta)$  is indicative of a material characterized by a high non-elastic strain component, and vice versa.

DMA tests were carried out through a DMA analyzer according to the suggestion of [9], based on an experimental program comprising of 3 tests in single cantilever configuration and 3 tests in three-point bending configuration.

TGA is an experimental technique, which provides the weight or the mass of a sample, measured as a function of temperature or time in isothermal experiments. The TGA measurements are commonly depicted as a TGA curve, in which the mass is plotted versus temperature or time. TGA tests were carried out through a thermobalance with horizontal arrangement, based on the experimental program comprising of 3 tests in Nitrogen ( $N_2$ ) atmosphere and 3 tests in air.

The results of DMA and TGA were processed using several techniques (Figure

1 and Figure 2. Outcomes are discussed more in depth in [11].  $T_g$  values range between 160°C ( $T_{g,offset}$ ) and 220°C ( $T_{g,max(tan\delta)}$ ) and  $T_d$  values range between 315°C ( $T_{d,offset}$ ) and 360°C ( $T_{g,midpoint}$ ). These results highlight that standardization of the test methods and processing are needed.

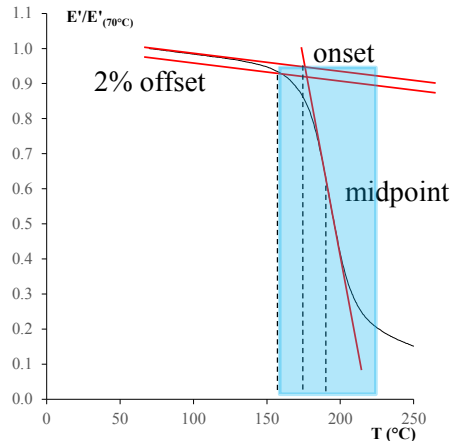


Figure 1 DMA processing methods

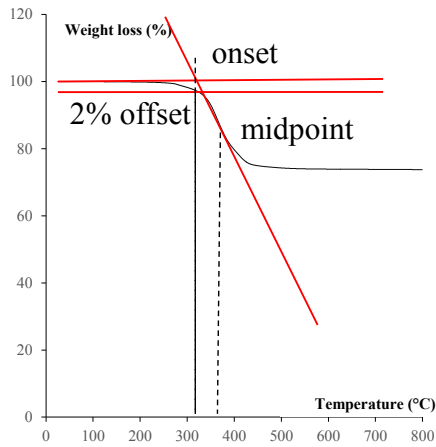


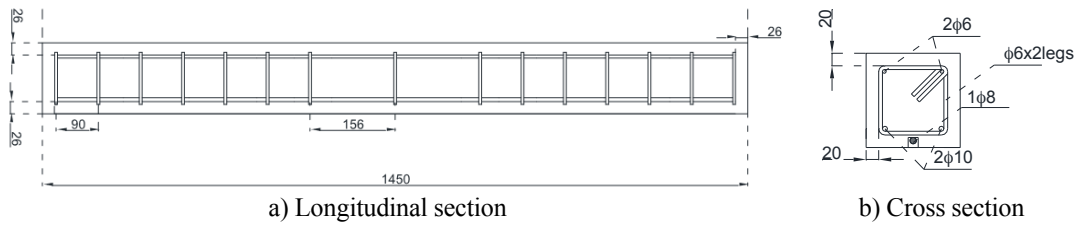
Figure 2 TGA processing methods

Tests on the cementitious grout adhesive yielded thermal conductivity values almost constant in the temperature range 50-175°C and equal to 0.55 W/mK; a slightly higher value (0.66 W/mK) was obtained at about 100°C, likely due to the evaporation of water, which led to a greater energy absorption than that needed to maintain a certain gradient of temperature in the sample, at other testing temperatures.

The mechanical properties of the constituent materials were also obtained through standard tests. The concrete compressive and tensile strength at 28 days is respectively 35.6 MPa and 3.83 MPa. The concrete compressive strength at 76 days is 47.7 MPa. The steel yield strength (rebars in tension side) is 525 MPa. The steel ultimate strength (rebars in tension side) is 622 MPa. The steel yield strength (rebars in compression side) is 700 MPa. The cementitious mortar compressive strength at 28 days is 90 MPa. The CFRP tensile strength is 1750 MPa and its elastic modulus is 136000 MPa.

## Design and Fabrication

All twelve beams had a flexural reinforcement in the form of two steel rebars (nominal diameter of 10 mm) on the tension side and two rebars (nominal diameter of 6 mm) in compression (**Figure 3b**). The strengthening system consisted of a CFRP bar (nominal diameter of 8 mm), grouted through a cementitious mortar in a groove 16 mm square in cross-section, cut into the concrete cover of the beam. The shear reinforcement was designed to ensure that flexural failure would govern. Steel stirrups (nominal diameter 6 mm) spaced at 90 mm centres were used (**Figure 3a**). The design was performed in accordance with EN1992-1 [12] and ACI 318-08 [13]; the stirrup spacing provided by EN1992-1 was adopted.

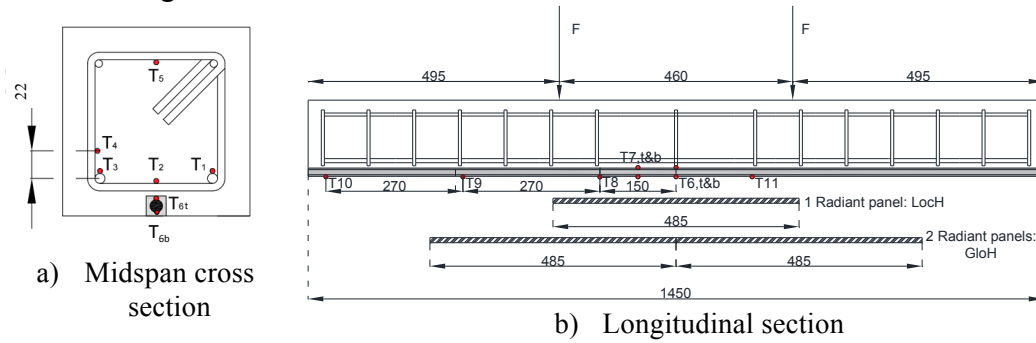


a) Longitudinal section  
 Figure 3 NSM FRP strengthened RC beam

After concrete casting and curing, the NSM strengthening system was applied. First, a wall chasing with two parallel diamond cutting discs was used to cut vertical slots in the bottom concrete cover of the beams. After finishing the working procedure, the remaining fin of the material was removed with a break-out tool. The groove was then made smooth and clean, and the bar was placed and grouted.

### Instrumentation and Test setup

Linear potentiometers were used to measure the vertical displacement at the beam midspan (LP100) and the bar's slip both at left hand side (LP25-LHS) and at right hand side (LP25-RHS) of the beams. A traditional strain gauge was also attached at the mid length of the CFRP bar. A high-resolution camera was set to take photos every five seconds during the tests. It enabled a digital image correlation (DIC) to monitor the vertical deflection and flexural strains of the beams. Thermocouples were located as shown in Figure 4.



b) Longitudinal section  
 Figure 4 Thermocouple locations

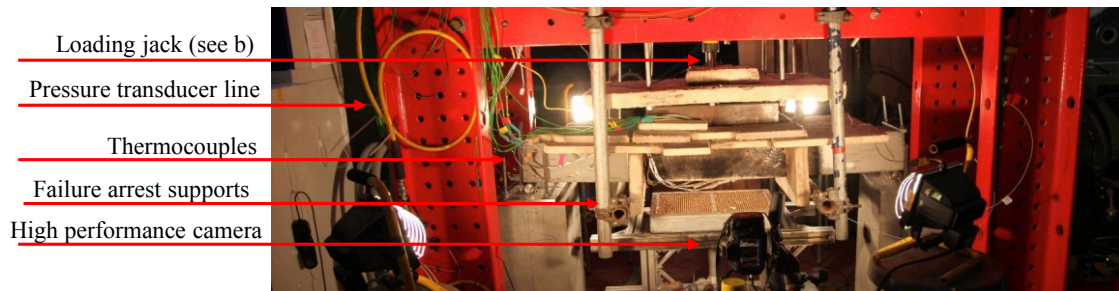


Figure 5 Flexural test setup (LocH configuration shown)

The tests in a local heating configuration (LocH) were carried out with a propane-fired radiant heating panel, with dimension of 485x330 mm, located at midspan 120 mm below the beams (Figure 5). The tests in global heating configuration (GloH) were carried out with two radiant heating panels, ensuring heating over the entire bonded length of the FRP system, which was 970 mm for the beams tested in this configuration.

## FLEXURAL TESTS RESULTS

### Ambient temperature

The flexural test of the strengthened beams showed that the beam cracked under a load of about 8 kN, as was also observed for un-strengthened beams. This means that the strengthening, as expected, does not significantly affect the pre-cracked moment of inertia. The load then linearly increased up to the yielding load, equal to about 56 kN (36% greater than the yielding load of the un-strengthened beams, corresponding to a midspan deflection of about 9 mm. After the steel yielding, the tensile loading of the CFRP bar led to slippage between FRP and the bonding agent. Then, the load increased up to about 59 kN (19% greater than the failure load of UN-S\_1), with a significant increase of the midspan deflection, up to about 21, due to the complete debonding of the CFRP bar in the cementitious grout. After the debonding of the strengthening system, which occurred when the slip of the bar on the right hand side (RHS) achieved about 6 mm, the strengthened beams showed a behaviour similar to that exhibited by the un-strengthened beam. Beam 'failure' occurred due to the concrete crushing. The strain in the CFRP bar, after the concrete cracking, linearly increased up to 5170  $\mu\epsilon$ , until bar slippage initiated. During the debonding stage the strain in the bar increased up to about 5850  $\mu\epsilon$ , corresponding to a slight increase in load. Finally, when the slip of the bar on RHS achieved about 6 mm, the load and the strain decreased due to the failure of the strengthening system. Additional information regarding ambient temperature tests can be found in [15].

### Elevated temperature

The elevated temperature tests highlighted the efficiency of the strengthening system, both in global and local heating configurations. Obviously, the effectiveness of the strengthening system during a fire event and its residual strength depends also on the utilization factor of the member in fire,  $\eta_{fi}$ , which is the ratio between the relevant effects of actions in the fire situation at time  $t$ ,  $E_{d,fi,t}$ , and the design value of the resistance of the member in the fire situation at beginning of thermal transience,  $R_{d,fi,0}$  (EN1991-1-2 [14]). The tests in global heating, undertaken on beams with a utilization factor equal to about 0.7 (sustained load of 40 kN), showed that the attainment of  $T_{d,midpoint}$  (360°C in Figure 6) along the overall bonded length of the CFRP bar led to debonding and subsequent loss of the effectiveness of the strengthening system. Nevertheless, the beam did not fail after 90 min of heating exposure since the un-strengthened beam, which was not affected by the strength reduction due to high temperature, carried the load even though it exhibited very large deflections (Figure 8). The residual tests confirmed that the residual failure load was equal to that obtained from testing the un-strengthened beams at ambient temperature.

The strengthening system of the tested beams with  $\eta_{fi}$  equal to about 0.7 tested in a local heating configuration did not fail after 90 min of fire exposure, even though the temperature of the CFRP bar in the heated zone was about 600°C (Figure 7). Note that this is a significantly higher temperature than the decomposition temperature of the polymer matrix of the bar. This means that the



CFRP bar in the heated zone was completely debonded. It is very likely that, due to the longitudinal thermal conductivity of the CFRP, the bar may have achieved the glass transition temperature close to the exposed zone. However, the effective cold-end anchorage was able to carry the stress transferred from midspan. Based on the results of bond tests performed at ambient temperature, presented in [15], and on the measurement of the maximum mechanical strains in the CFRP bars during tests on LocH-SL<sub>i</sub> beams, the effective end-anchorage length could have been just 300 mm to avoid the failure. Figure 8 shows deflection versus time, highlighting that in a local heating configuration the deflection of the beams was significantly lower than that observed in global heating, since the thermal gradient and therefore the thermal curvature were lower than that induced by global heating.

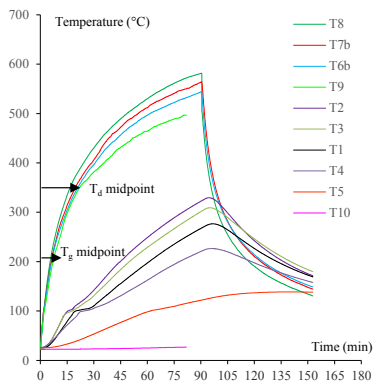


Figure 6 Temperature recorded by thermocouples (GloH)

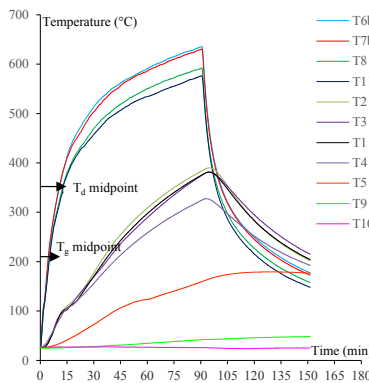


Figure 7 Temperature recorded by thermocouples (LocH)

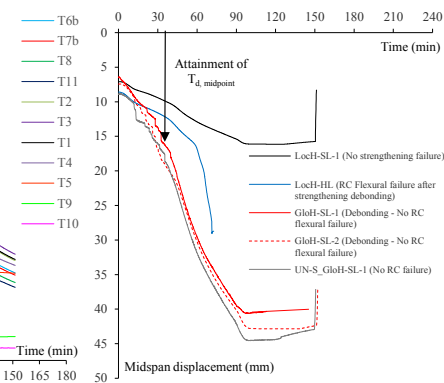


Figure 8 Midspan displacement versus time

Finally, the strengthening of the beams tested in a local heating configuration with  $\eta_{fi}$  equal to about 0.8 (sustained load of 50 kN), was unable to sustain the stress transferred from midspan when the maximum temperature in the CFRP bar near midspan achieved about 600°C, even if the temperature at the end-anchorage was effectively at ambient temperature. As previously noted, it is very likely that the CFRP bar close to the exposed zone may have achieved the glass transition temperature, leading to a reduction of effectiveness of the end-anchorage.

The tests showed the importance of a cold end-anchorage zone to maintain the load bearing capacity of the strengthening in case of fire, especially under sustained loads typical of maximum service strain conditions in the FRP. It is noteworthy that the tensile strength of the CFRP bar was never attained, although (i) a significant temperature (more than 600°C) was attained in the bar during the heating phase, and (ii) a significant sustained stress was present due to sustained load.

## CONCLUSIONS

The tests presented in this paper, on the novel cementitious-bonded CFRP NSM strengthening system specifically developed to address the problematic performance of conventional epoxy adhered FRP strengthening systems at elevated temperatures, show that:

- DMA yielded a  $T_g$  ranging between 160°C ( $T_{g,offset}$ ) and 220°C ( $T_{g,max(tan\delta)}$ ). TGA provided  $T_d$  values ranging between 320°C ( $T_{d,offset}$ ) and 360°C ( $T_{d,midpoint}$ ). All these variabilities in results, highlight the importance to standardize  $T_g$  and  $T_d$  definition as well as the test setup configuration.

- the cementitious-bonded NSM FRP strengthening system is able to sustain loads typical of service conditions also at elevated temperatures up to 600°C.
- the capacity of the novel NSM FRP system depends on the presence of effective cold anchorage, because carbon fibres behave significant strength also at elevated temperature even when the performance of the polymer matrix is compromised.
- local insulation systems placed at the end-anchorage only, instead of insulation along the overall bonded length for the FRP system, may be able to prolong overall system performance in fire.

It should be noted that an investigation about the correlation between the debonding of the bar and the attainment of its glass transition temperature in the anchorage zone is still in progress. The results of this study will be presented in the future as further development of this research.

## ACKNOWLEDGEMENT

The authors would like to thank Milliken for providing the FRP materials and cementitious mortar (marketed under the trade name FireStrong) used in the experimental program.

## REFERENCES

1. Yu B., Kodur V., (2014). Fire behavior of concrete T-beams strengthened with near-surface mounted FRP reinforcement. *Engineering Structures*. 2014;80:350-361.
2. El-Gamal S., Al-Salloum Y., Alsayed S., Aqel M., (2012). Performance of near surface mounted glass fiber reinforced polymer bars in concrete. *Journal of Reinforced Plastics and Composites*, 31 (22) 1501–1515 DOI: 10.1177/073168441246408
3. Petri P., Blaszk G., Rizkalla S., (2013). Structural Fire Endurance of an RC Slab Strengthened with High T<sub>g</sub> Near Surface Mounted CFRP Bars. ACIC 2013, Edited by Miss Claire. J. Whysall and Prof. Su. E. Taylor, 140-151, Queen's University Belfast on 10 -12 September 2013
4. Burke P.J., Bisby L. A., Green M., (2013). Effects of elevated temperature on near surface mounted and externally bonded FRP strengthening systems for concrete. *Cement & Concrete Composites* 35 (2013) 190–199
5. Palmieri A., Matthys S., Taerwe L., (2013). Fire Endurance and Residual Strength of Insulated Concrete Beams Strengthened with Near-Surface Mounted Reinforcement. *J. Compos. Constr.* 2013.17:454-462
6. El-Hacha R., Rizkalla S: H., (2004). Near-Surface-Mounted Fiber-Reinforced Polymer Reinforcements for Flexural Strengthening of Concrete Structures, *ACI Structural Journal*, September-October 2004, 717-726
7. Foret G., Limam O., (2008). Experimental and Numerical analysis of RC two-way slabs strengthened with NSM CFRP rods, *Construction and Building Materials* 22 (2008) 2025-2030
8. Bilotta A., Ceroni F., Di Ludovico M., Nigro E., Pecce M., (2011). Bond Efficiency of EBR and NSM FRP Systems for Strengthening Concrete Members, *J. Compos. Constr.* 2011.15:757-772
9. ISO 6721-1:2011. *Plastics - Determination of dynamic mechanical properties - Part 1: General principles*
10. ASTM D 4092 – 07 (2013). *Standard Terminology for Plastics: Dynamic Mechanical Properties*
11. Del Prete I., Bilotta A., Bisby L., Nigro E., (2015). NSM FRP strengthened reinforced concrete beams: Benefits in fire of high T<sub>g</sub> FRP & cementitious adhesive. *Applications of Structural Fire Engineering*, 15-16 October 2015, Dubrovnik, Croatia, 331-336
12. EN1992-1-1 (2004). *Eurocode 2: Design of concrete structures - Part 1-1: General rules and rules for buildings*
13. ACI 318-08 (2009). *Building Code Requirements for Structural Concrete*. ACI Committee 318, American Concrete Institute
14. EN1991-1-2 (2002). *Eurocode 1: Actions on structures – Part 1-2: General actions – Actions on structures exposed to fire*
15. Del Prete I., Bilotta A., Bisby L., Nigro E., (2015). Bond tests on NSM FRP strengthening using cementitious matrices for concrete structures. FRPRCS-12 & APFIS-2015 Joint Conference, 14-16 December 2015, Nanjing, China